ARCHIVES
of
FOUNDRY ENGINEERING

DOI: 10.2478/afe-2013-0026

Published quarterly as the organ of the Foundry Commission of the Polish Academy of Sciences

VERSITA

ISSN (2299-2944)
Volume 13
Issue 1/2013

134 – 140

Application of Averaged Voronoi Polyhedron in the Modelling of Crystallisation of Eutectic Nodular Graphite Cast Iron

A.A. Burbelko*, J. Początek, M. Królikowski
Department of Cast Alloys and Composites Engineering, Faculty of Foundry Engineering,
AGH University of Science and Technology, Al. A. Mickiewicza 30, 30-059 Cracow, Poland
* Corresponding author. E-mail address: abur@agh.edu.pl

Received 15.07.2012; accepted in revised form 04.09.2012

Abstract

The study presents a mathematical model of the crystallisation of nodular graphite cast iron. The proposed model is based on micro- and macromodels, in which heat flow is analysed at the macro level, while micro level is used for modelling of the diffusion of elements. The use of elementary diffusion field in the shape of an averaged Voronoi polyhedron [AVP] was proposed. To determine the geometry of the averaged Voronoi polyhedron, Kolmogorov statistical theory of crystallisation was applied. The principles of a differential mathematical formulation of this problem were discussed. Application of AVP geometry allows taking into account the reduced volume fraction of the peripheral areas of equiaxial grains by random contacts between adjacent grains.
As a result of the simulation, the cooling curves were plotted, and the movement of "graphite-austenite" and "austenite-liquid" phase boundaries was examined. Data on the microsegregation of carbon in the cross-section of an austenite layer in eutectic grains were obtained. Calculations were performed for different particle densities and different wall thicknesses. The calculation results were compared with experimental data.

Keywords: Cast iron with nodular graphite, Modelling, Averaged Voronoi polyhedron

1. Introduction

Because of its outstanding mechanical and casting properties, the nodular graphite cast iron is a very important material used in industry [1]. The properties of this cast iron result mainly from the microstructure that is formed during crystallisation. One of the important parameters affecting the microstructure is the graphite nodules size and count. It affects the kinetics of phase transformations during crystallisation and cooling, and also during the process of the possible heat treatment of castings.

Recently, a significant increase of the interest in thin-walled castings made of nodular graphite cast iron has been observed [2]. Castings made of this material not only have a low weight, but also very good mechanical properties [3-5]. For this reason, nodular graphite cast iron continues being the object of studies using different mathematical models, the main task of which is the best approximation of processes that occur during crystallisation of this alloy [6-10].

The number of mathematical models allowing the simulation of solidification process in a foundry mould has grown quite

considerably. Due to the continuous increase of computing power, today's models are not limited only to the description of heat flow in a casting-mould system, using the Fourier-Kirchhoff equation (macromodels) [11], but also allow modelling of, among others, microstructure and segregation of alloying elements (micro-macro models) [12-14]. This is very important for thin-walled castings, as the short cooling time prevailing in such objects does not allow the chemical composition to become homogeneous within the crystallised austenite grains.

The subject and aim of this study is to create a mathematical model describing the field of carbon concentration in an aspherical elementary diffusion field (EDF) during the crystallisation of eutectic nodular graphite cast iron and after its solidification. The model assumes that as a result of random contacts between the eutectic grains growing around the individual nodules of graphite, EDF has an aspherical shape.

To determine the geometry of a three-dimensional EDF, the principles of the statistical theory of crystallisation have been used in this study [15].

2. Model of nodular graphite cast iron crystallisation

2.1. Heat flow

To determine the cooling rate of a thin-walled casting poured in sand mould, Fourier equation was applied:

$$c\frac{\partial T}{\partial \tau} = \nabla(\lambda \nabla T) + q_T \tag{1}$$

where: T - temperature, τ - time, λ - thermal conductivity, c - specific heat, q_T - function of heat source (the intensity of the evolution of the latent heat of crystallisation).

To solve equation (1), the finite difference method (FDM) was used, allowing for the one-dimensional heat flow. The heat source function takes values different from zero only in the casting, which confers to equation (1) a non-linear character. To determine its value, the following relationship was used:

$$q_T = L\frac{\partial f}{\partial \tau} \tag{2}$$

where: L – the volumetric heat of phase transformations, ∂ f - the speed of increase of the solidified phase content in a time step.

The numerical calculations neglected the temperature variations in the thin-walled casting cross-section (using appropriate step of FDM in the casting), but included the heat flow resistance at the “casting-mould” phase boundary.

2.2. Diffusion

Currently, only carbon diffusion is analysed in the model. The concentration field of this element is determined in the austenite envelope surrounding the nodule of graphite and in the liquid matrix using the following equation:

$$\frac{\partial C}{\partial \tau} = div\left(D_f \cdot grad(C)\right) \tag{3}$$

where: D - diffusion coefficient, C – carbon concentration in a given phase.

As an initial condition for the modelling it has been assumed that, according to the stoichiometric composition of the eutectic, in the middle of an EDF filled with the liquid phase there is a graphite nodule of a 1.0 μm radius surrounded by the austenite envelope 1.4 μm thick [16]. Equation (3) is solved separately for the austenite envelope and for the liquid, adopting the following conditions determined from the Fe-C phase equilibrium diagram:

- concentration in austenite at the graphite phase boundary:

$$C_{\gamma/gr} = 3.3658\cdot 10^{-5}T - 1.8036542\cdot 10^{-2} \tag{4}$$

- concentration in austenite at the liquid phase boundary:

$$C_{\gamma/L} = -5.2525254\cdot 10^{-5}T + 8.141414\cdot 10^{-2} \tag{5}$$

- concentration in liquid at the austenite phase boundary:

$$C_{L/\gamma} = -9.881423\cdot 10^{-5}T + 1.566316\cdot 10^{-1} \tag{6}$$

On the external EDF border, an adiabatic boundary condition was assumed.

2.3. Differential approximation and EDF geometry – averaged Voronoi polyhedron

For a description of polycrystalline structures in computational tasks, Voronoi polyhedrons are often used. To a system of "nuclei" of an arbitrary spatial distribution respective of the polyhedron (i.e. the grain) related with this system shall belong all the space points that lie closer to this "nucleus" than to any other. The walls of this polyhedron are fragments of planes perpendicular to the segments joining the "nuclei" and dividing these segments into two equal parts. The specific shape and volume of this polyhedron, as well as the number of faces and edges depend on the distribution of the nearest neighbouring "nuclei". Structure of this type is formed in the case of an immediate nucleation of the grains and their spherical growth at an equal rate. In this study, to solve equation (3), the elementary balance method was used. Numerical calculations were performed

for the area of an averaged Voronoi cell. The method to determine the geometry of EDF and equations used in the solution are shown below.

In the modelling it has been assumed that within the area of EDF, at any arbitrary time instant, carbon concentration can be described as a product of two functions:

$$C(r,\tau) = f(r)\cdot\theta(\tau) \tag{7}$$

It means that the diffusion fluxes in EDF are directed radially with respect to the centre, while the side flux is neglected. A zero diffusion flux through the Voronoi cell boundary was also adopted.

According to [15], in the case of an immediate nucleation of the *n* grains present in a unit volume and their spherical growth at the same (not necessarily constant) speed, the volume of the material at a maximum distance *r* from the nucleation site can be determined by the following equation:

$$V(r) = \frac{1}{n}\left(1-\exp\left(-\frac{4}{3}\pi n r^3\right)\right) \tag{8}$$

The field of the surface separating the area $V(r)$ from the material more remote from the nucleation site is:

$$F(r) = \frac{dV(r)}{dr} = 4\pi r^2\cdot\exp\left(-\frac{4}{3}\pi n r^3\right) \tag{9}$$

The volume of the material area whose distance from the nucleation site is comprised in the range from *r* to $(r + \Delta r)$ can be computed as:

$$\Delta V(r,\Delta r) = \frac{1}{n}\left\{\exp\left(-\frac{4}{3}\pi n r^3\right)-\exp\left[-\frac{4}{3}\pi n(r+\Delta r)^3\right]\right\} \tag{10}$$

or for $\Delta r << r$:

$$\Delta V(r,\Delta r) \approx 4\pi r^2\Delta r\exp\left(-\frac{4}{3}\pi n r^3\right) \tag{11}$$

In this case, the difference equation for the elementary balance method can be written as:

$$\Delta V(r_1,\Delta r)\cdot\frac{C(r,\tau+\Delta\tau)-C(r,\tau)}{\Delta\tau} = D(r_1)\cdot grad[C(r_1)]\cdot F(r_1) - D(r_2)\cdot grad[C(r_2)]\cdot F(r_2) \tag{12}$$

where: $D(r)$ – average diffusion coefficient of material in a layer of EDF; $r_2 = r_1 + \Delta r$, $r = (r_1+r_2)/2$.

If the concentration gradient is approximated with the central differential quotient and the explicit scheme is used, then in the case of constant grid step Δr the concentration in the *i* area of an elementary balance can be computed as:

$$C_i(\tau+\Delta\tau) = (1-A_i-B_i)\cdot C_i(\tau) + A_i C_{i-1}(\tau) + B_i C_{i+1}(\tau) \tag{13}$$

where:

$$A_i = \frac{D(r_i)\cdot F(r_i)\cdot\Delta\tau}{\Delta V(r_i,\Delta r)\cdot\Delta r},\quad B_i = \frac{D(r_i+\Delta r)\cdot F(r_i+\Delta r)\cdot\Delta\tau}{\Delta V(r_i,\Delta r)\cdot\Delta r} \tag{14}$$

It has been assumed that the *i* area is located within the distance range of r_i to $r_i+\Delta r$ from the centre of EDF.

The Voronoi polyhedron is convex but not necessarily bounded [17]. From equation (8) it follows that the fraction of the EDF space distant from the centre by a value exceeding R_m is:

$$f(R_M) = \exp\left(-\frac{4}{3}\pi n R_M^3\right) \tag{15}$$

Assuming a small value of this fraction, further called the rounding constant, the EDF radius for which the calculations are to be performed can now be determined:

$$R_M = \sqrt[3]{-\frac{3\ln f}{4\pi n}} \tag{16}$$

According to [13], $f = 1\cdot10^{-3}$ has been adopted.

2.4. Phase boundaries

The calculations were performed on a differential grid with constant space step (with the exception of boundary elements in areas adjacent to the phase boundaries). In boundary elements, along the sections EDF with a length of $2\Delta r$ involving the interfaces between adjacent phases, a variable spatial step has been used with the interface between adjacent balance elements overlapping the phase boundary. The width of the boundary elements varies in the range from $0.5\cdot\Delta r$ to $1.5\cdot\Delta r$. When this range is exceeded, the calculation grid is subjected to local modifications to move the boundary elements, while preserving the mass balance of constituents.

The speed of the "graphite-austenite" and "austenite-liquid" phase boundaries migration is determined from the mass balance at interfaces:

$$u_{\gamma/gr}\left(C_{gr}\rho_{gr} - C_{\gamma/gr}\rho_\gamma\right) = -D_\gamma\rho_\gamma\left.\frac{dC_\gamma}{dr}\right|_{r_{gr}^+} \tag{17}$$

$$u_{L/\gamma}\left(C_{L/\gamma}\rho_L - C_{\gamma/L}\rho_\gamma\right) = D_\gamma \rho_\gamma \left.\frac{dC_\gamma}{dr}\right|_{r_{gr}^-} - D_L \rho_L \left.\frac{dC_\gamma}{dr}\right|_{r_{gr}^-} \quad (18)$$

where: $u_{\gamma/gr}$ – the migration speed of the „austenite-graphite" interface (the graphite growth rate); $u_{L/\gamma}$ – the migration speed of the „austenite-liquid" interface (the eutectic grain growth rate).

3. Modelling conditions

Calculations were performed for cast plates 3 and 5 mm thick, poured in sand moulds.

The thermophysical parameters used in modelling are shown in Table 1. The initial temperature was 1595 K and 298 K for the metal and mould, respectively.

Table 1.
The thermophysical parameters used in modelling

Thermal conductivity: W/(m·K)			Reference
– liquid	λ_L	30	[19]
– austenite	λ_γ	20	[20]
–graphite	λ_{gr}	20	[20]
Carbon diffusion coefficient in: m^2/s			
– liquid	D_L	$1.25 \cdot 10^{-9}$	[21]
Enthalpy of phase transformations: J/m^3			
– liquid into austenite	$\Delta H_{L\rightarrow\gamma}$	$19.71 \cdot 10^8$	[20]
– liquid into graphite	$\Delta H_{L\rightarrow gr}$	$16.16 \cdot 10^5$	
– austenite into graphite	$\Delta H\gamma\rightarrow gr$	$8.8 \cdot 10^5$	
Specific heat: $J/(m^3 \cdot K)$			
– liquid	$c_{v,L}$	$5.6 \cdot 10^6$	[20]
– austenite	$c_{v,\gamma}$	$5.84 \cdot 10^6$	[19]
–graphite	$c_{v,gr}$	$17.84 \cdot 10^5$	[20]
Density: kg/m^3			
– liquid	ρ_L	$7 \cdot 10^3$	[22]
– austenite	ρ_γ	$7.3 \cdot 10^3$	[19]
–graphite	ρ_{gr}	$2.23 \cdot 10^3$	[20]

The initial carbon content in the liquid phase of an Fe-C alloy amounted to 0.0426 of the weight fraction. In the calculations of carbon diffusion, a spatial grid step of 1 μm was used.

The value of the diffusion coefficient in austenite was adopted as a variable in function of temperature according to [18]:

$$D_\gamma = 1.67 \cdot 10^{-2} \exp\left(-\frac{1.2 \cdot 10^5}{R \cdot T}\right) \quad (19)$$

where: R = 8.3144621 J/(mole·K), T – absolute temperature, K.

Table 2 shows the dimensions of EDF used in the simulation, based on the number of grains calculated in accordance with (16). The model assumed an instantaneous nucleation of eutectic grains. Calculations were performed for the number of grains obtained in experimental castings, and for two close values (see Table 2).

Table 2.
Radii of the elementary diffusion field

Casting thickness, mm	Grain density, m^{-3}	EPD radius, μm
3	$5 \cdot 10^{14}$	18
	$9.7 \cdot 10^{14}$	15
	$1 \cdot 10^{15}$	14
5	$1 \cdot 10^{13}$	65
	$3.8 \cdot 10^{14}$	42
	$1 \cdot 10^{14}$	31

4. Results of modelling

Figure 1 compares the cooling curves obtained by modelling with the curve obtained experimentally for castings of two wall thicknesses.

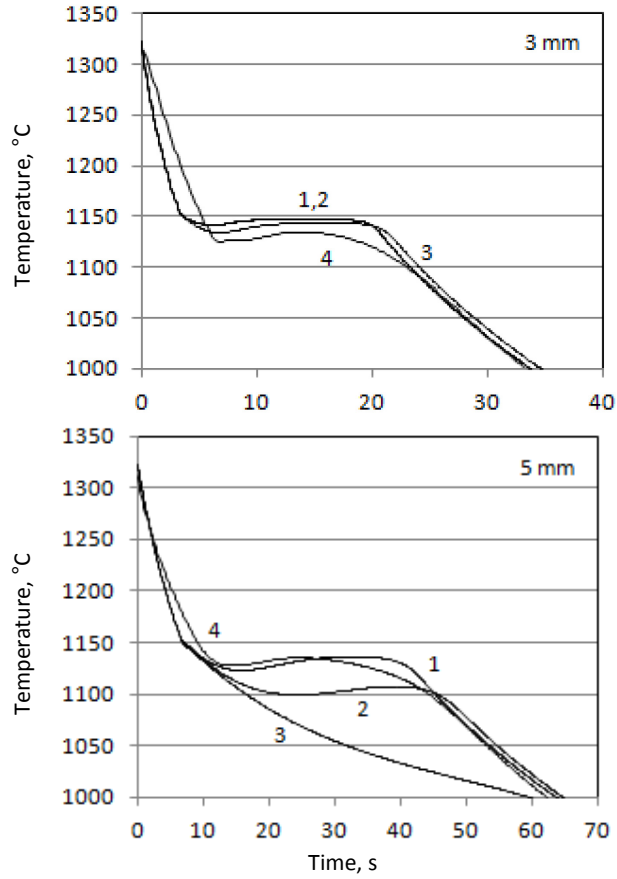

Fig. 1. Fragments of the casting cooling curves. The results of simulation obtained for the following eutectic grain densities: casting wall thickness: 3 mm: 1 - $n=10^{15}$, 2 - $n=9.7 \cdot 10^{14}$, 3 - $n=5 \cdot 10^{14}$ m^{-3}; casting wall thickness: 5 mm: 1 - $n=10^{14}$, 2 - $n=3.8 \cdot 10^{13}$, 3 - 10^{13} m^{-3}; 4 – the result of measurement.

Changes in the distance of the "graphite-austenite" and "austenite-liquid" phase boundaries from the centre of eutectic grain are shown in Figure 2, while Figure 3 shows an increase in

the volume fraction of graphite and austenite. As can be seen from these figures, the increasing speed of migration of the "austenite-liquid" phase boundary before the end of solidification does not increase the speed of volume changes.

The heterogeneity of carbon concentration in the cross-section of an austenite layer in the EDF at the end of crystallisation is shown in Figure 4. The heterogeneity of chemical composition of the metal matrix has an impact on the course of phase transformations in solid state and on the formation of final microstructure in casting.

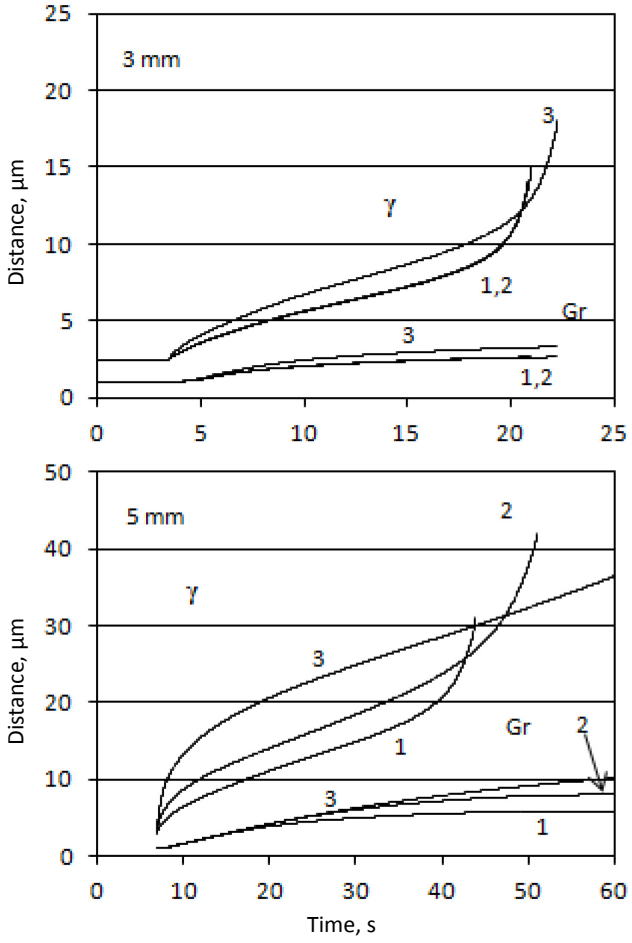

Fig. 2. Changes in the position of „graphite-austenite" (Gr) and „austenite-liquid" (γ) phase boundaries in castings with the wall thickness of 3 mm (the densities of eutectic grains: 1 - $n=10^{15}$, 2 - $n=9.7\cdot10^{14}$, 3 - $n=5\cdot10^{14}$ m^{-3}) and 5 mm (the densities of eutectic grains: 1 - $n=10^{14}$, 2 - $n=3.8\cdot10^{13}$, 3 - 10^{13} m^{-3}) – the results of simulation

The known mathematical models of diffusion fields in a eutectic grain of the nodular graphite cast iron assume a spherical symmetry of EDF [23]. In this field, the volume fraction of metal matrix increases with increasing distance from the graphite grain.

For an averaged Voronoi cell, the probability that a random point in the structure of eutectic grain will be located at a distance from the nucleus centre smaller than r is described with a cumulative distribution function:

$$P(r)=1-\exp\left(-\frac{4}{3}\pi n r^3\right) \tag{20}$$

The probability density function

$$p(r)=4\pi n r^2\cdot\exp\left(-\frac{4}{3}\pi n r^3\right) \tag{21}$$

has its maximum at the point

$$R_{VP}=(2\pi n)^{-1/3} \tag{22}$$

The value of R_{VP} can be called a characteristic radius of the averaged Voronoi polyhedron. Among the random points selected in the sample volume composed of Voronoi polyhedra, the points located at a distance R_{VP} from the nucleus centre will occur at maximum frequency. In addition, according to (21), at a distance from the nucleus centre not exceeding the value of R_{VP} will be located 48.7% of the grains volume, while the fraction of an area lying at a distance larger than $2\cdot R_{VP}$ from the centre will amount to less than 0.5%. These values for the examined density of grains are summarised in Table 3.

Theoretically, in a Voronoi cell, the maximum distance of a point from the centre is not limited [17], but according to (22), the probability of occurrence of the areas where this distance would increase to a value above $2\cdot R_{VP}$ rapidly decreases to zero.

Carbon concentration changing along the radius of an austenite envelope after the end of crystallisation is shown in Figure 5. In this figure, concentrations are indicated at points located at a distance of one and two characteristic radii from the centre of the grain. The concentration of carbon higher than at the point distant by $2\cdot R_{VP}$ from the grain centre may occur in less than 0.5% of the alloy volume and, according to equation (22), with increasing concentration the probability of its occurrence rapidly decreases.

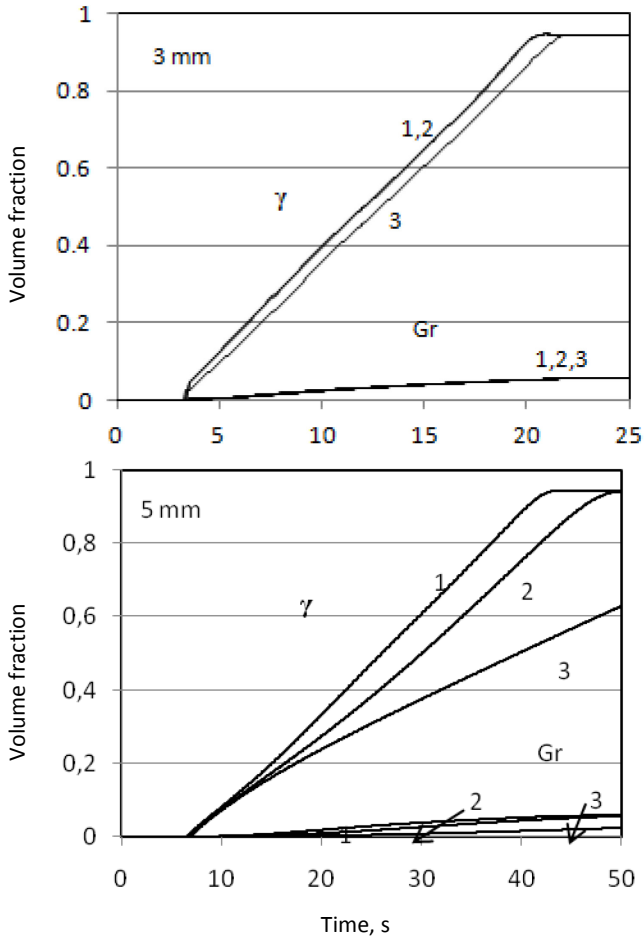

Fig. 3. Changes in the volume fraction of graphite (Gr) and austenite (γ) in castings with the wall thickness of 3 mm (the densities of eutectic grains: 1 - n=10^{15}, 2 - n=$9.7\cdot10^{14}$, 3 - n=$5\cdot10^{14}$ m^{-3}) and 5 mm (the densities of eutectic grains: 1 - n=10^{14}, 2 - n=$3.8\cdot10^{13}$, 3 - 10^{13} m^{-3}) – the results of simulation

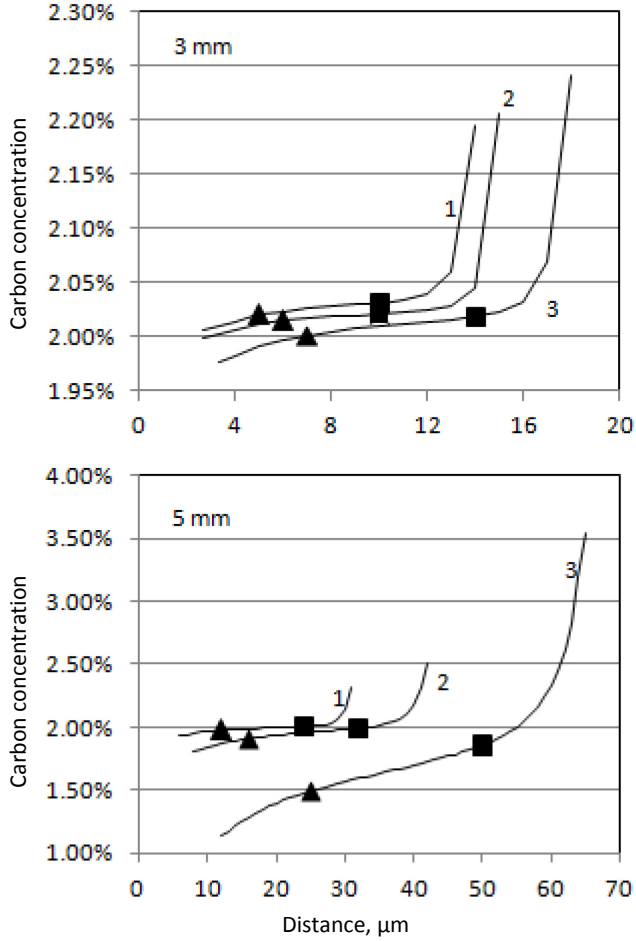

Fig. 4. Changes of carbon concentration in austenite along the EDF radius in castings with the wall thickness of 3 mm (the densities of eutectic grains: 1 - n=10^{15}, 2 - n=$9.7\cdot10^{14}$, 3 - n=$5\cdot10^{14}$ m^{-3}) and 5 mm (the densities of eutectic grains: 1 - n=10^{14}, 2 - n=$3.8\cdot10^{13}$, 3 - 10^{13} m^{-3}); ▲– the concentration at a distance R_{VP} from the grain centre, ■ – the concentration at a distance $2\cdot R_{VP}$ from the grain centre

Table 3.
Characteristic radii of the averaged Voronoi polyhedrons

Grain density, m^{-3}	R_{VP}, μm	$2\cdot R_{VP}$, μm
10^{13}	25,1	50,3
$3.8\cdot10^{13}$	16,1	32,2
$1\cdot10^{14}$	11.7	22.4
$5\cdot10^{14}$	6.8	13.6
$9.7\cdot10^{14}$	5,5	11.0
10^{15}	5,4	10,8

5. Conclusions

A mathematical model of carbon diffusion in a eutectic grain during the crystallisation of nodular graphite cast iron was developed. As a geometry of the elementary diffusion field, an averaged Voronoi cell was adopted.

The solidification of eutectic cast iron with nodular graphite in castings with the walls of 3 and 5 mm thickness was simulated. The cooling curves were obtained which are qualitatively consistent with the typical cooling curves plotted for thin-walled castings made from the nodular graphite cast iron.

The distribution of carbon concentration values in an austenite envelope along the eutectic grain radius was disclosed.

Acknowledgements

Studies were carried out under the statutory AGH research programme No. 15.11.170.449.

References

[1] 45th Census of World Casting Production. Staff Report. Modern Casting, December 2011, 16-18.
[2] Górny, M. (2010). *Kształtowanie struktury supercienkościennych odlewów z żeliwa sferoidalnego.* Kraków. Wydawnictwo Naukowe AKAPIT.
[3] Fraś, E., Górny, M. & Lopez HF.(2009). Thin wall ductile and austempered iron castings as substitutes for aluminum alloy castings. *International Foundry Research / Giesserei-forschung.* 61(3), 2-10.
[4] Fraś, E., Górny, M. & Lopez, HF. (2008). Thin wall ductile and austempered iron castings. *AFS Transactions*. 116, 601-610.
[5] Stefansecu, D.M., Ruxanda, R.E. & Dix, L.P. (2003). The metllurgy and ten sile mechanical properties of thin wall spheroidal graphite irons. *Int Journal of Cast Metals Res*. 16, 319-324.
[6] Su, K. et al. (1985) Computer simulation of solidification of nodular cast iron. *The Physical Metallurgy of Cast Iron*, *v. 34*, Elsevier Sci. Publ. Co., North-Holland. 181-190.
[7] Stefanescu, D.M., Catalina, A., Guo, X., Chuzhoy, L., Pershing, M.A. & Biltgen, G.L. (1998). Prediction of room temperature microstructure and mechnical properties in iron castings. Modeling of Casting, Welding and Advanced Silidification Process - VIII, ed. B.G. Thomas, C. Beckermann, TMS. 455-459.
[8] Yoo, S. M., Ludwig, A. & Sahm, P.R. (1997). Numerical simulation of nodular cast iron in permanent moulds. Solidification Processing. *Renmour House, Univ. of Sheffield*. 494-497.
[9] Liu, J. & Elliott, R. (1998). Numerical model for microsegregation in ductile iron. *Materials Science and Technology*. 14, 1127-1131.
[10] Onsoien, M.I., Grong, O., Gundersen, O. & Skaland, T. (1999). A process model for the microstructure evolution in ductile cast iron: Part 1. the Model. *Metallurgical and Materials Transactions.* 30A, 1053-1068.
[11] Burbelko, A.A., Gurgul, D., Kapturkiewicz, W., Początek, J. & Wróbel, M. (2011). Cellular automaton modeling of ductile iron microstructure in the thin wall. *Archives of Foundry Engineering*. 11(1), 13-18.
[12] Fraś, E., Kapturkiewicz, W. & Burbelko, A.A. (1997). Computer modeling of primary structure formation in ductile iron. *Advanced Materials Research.* Scitech Publications, Switzerland. 4-5. 499-504.
[13] Fraś, E., Kapturkiewicz, W. & Lopez, H. (1992). Macro and micro modeling of the solidification kinetics of cast iron. *Trans. AFS.* 100, 583-591.
[14] Lee, P.D. & Chirazi, A. (2002). Multiscale computational modeling of solidification phenomena. *Physics Reports-Review Section of Phys. Lett.* 365, 145-249.
[15] Kolmogorov, A.N. (1937). On the Statistical Theory of Metal Crystallisation. *Bull. Acad. Sci*. USSR. 3, 355-359.
[16] Wetterfal, S., Fredriksson, H. & Hillert, M. (1972). Solidification process of nodular cast iron. *Journal iron steel institute*. 5, 323-333.
[17] Brostow, W. & Castano, V.M. (1999). Voronoi polyhedra as a tool for dealing with spatial structures of amorphous solids, liquids and dense gases. *Journal of Materials Education*. 21, 297-304.
[18] Burbelko, A.A., Początek, J. & Królikowski, M. (2012). Zastosowanie wielościanu Voronoia w modelowaniu krystalizacji żeliwa z grafitem kulkowym. *Oddane do druku.*
[19] Beltran-Sanchez, L. & Stefanescu, D.M. (2004). A quantitative dendrite growth model and analysis of stability concepts. *Metall. and Materials Trans. A.* 35A, 2471-2485.
[20] Kikoin, I.K Ed. (1976). *Tabele wielkości fizycznych.* Moskwa, Avtomizdat.
[21] Magnin, P., Mason, J.T. & Trivedi, R. (1991). Growth of Irregular Eutectic and the Al-Si System. *Acta Metallurgia et Materialia*, 39(4), pp. 469-480.
[22] Fraś, E. (1992). *Krystalizacja metali i stopów*. Warszawa Wydawnictwo Naukowe PWN.
[23] Kapturkiewicz, W., Burbelko, A.A., Lelito, J. & Fraś, E., (2003). Modelling of ausferrite growth In ADI. *International Journal of Cast Metals Research*. 16, 287-292.
[24] Kapturkiewicz, W. (2003). *Modelowanie krystalizacji odlewów żeliwnych*, Kraków, Wydawnictwo naukowe AKAPIT.